Journal of Chromatography B, 867 (2008) 160–164

Contents lists available at ScienceDirect

Journal of Chromatography B

journal homepage: www.elsevier.com/locate/chromb

Short communication

Zinc-decorated silica-coated magnetic nanoparticles for protein binding and controlled release

Marjan Bele[a], Gorazd Hribar[a], Stanislav Čampelj[b], Darko Makovec[b], Vladka Gaberc-Porekar[a], Milena Zorko[a], Miran Gaberšček[a,*], Janko Jamnik[a], Peter Venturini[a]

[a] National Institute of Chemistry Slovenia, Hajdrihova 19, 1000 Ljubljana, Slovenia
[b] Jožef Stefan Institute, Jamova 39, 1000 Ljubljana, Slovenia

ARTICLE INFO

Article history:
Received 14 December 2007
Accepted 20 March 2008
Available online 29 March 2008

The paper is dedicated to the memory of Dr. Viktor Menart who played a crucial role in initiating this work.

Keywords:
Magnetic nanoparticles
Silica coating
Zinc adsorption
Histidine affinity binding
Protein binding
Protein nanoparticles
Coordinative binding

ABSTRACT

The aim of this study was to be able to reversibly bind histidine-rich proteins to the surface of maghemite magnetic nanoparticles *via* coordinative bonding using Zn ions as the anchoring points. We showed that in order to adsorb Zn ions on the maghemite, the surface of the latter needs to be modified. As silica is known to strongly adsorb zinc ions, we chose to modify the maghemite nanoparticles with a nanometre-thick silica layer. This layer appeared to be thin enough for the maghemite nanoparticles to preserve their superparamagnetic nature. As a model the histidine-rich protein bovine serum albumin (BSA) was used. The release of the BSA bound to Zn-decorated silica-coated maghemite nanoparticles was analysed using sodium dodecyl sulfate polyacrylamide gel electrophoresis (SDS-PAGE). We demonstrated that the bonding of the BSA to such modified magnetic nanoparticles is highly reversible and can be controlled by an appropriate change of the external conditions, such as a pH decrease or the presence/supply of other chelating compounds.

1. Introduction

Core-shell-type composites consisting of magnetic nanoparticles decorated with biological substances are interesting for various biomedical applications. Typical uses include magnetic resonance imaging contrast enhancement, bioseparation, biosensing, magnetofection, cancer therapy with magnetic hyperthermia, and targeted drug delivery. When designing such composites, the main aim has mostly been to immobilize a given bioactive substance on the surface with a sufficiently strong bond to ensure the composite's stability prior to and during the application. For certain applications, however, it would be desirable for the bonding of the biosubstance to the magnetic core to be reversible.

Recently, an interesting type of bead for binding histidine-tagged proteins [1], consisting of a magnetic core and a nickel–silica composite matrix with Ni (II) ions tightly integrated into the silica, has been described. The material has no spacers and contains no chelating compounds for the binding of the Ni (II) ions, but the result is still a large number of potential binding sites for protein histidines. However, a very high ligand density is not always advantageous. From the literature we know that the ligand density can affect the binding and separation capabilities in immobilized metal affinity chromatography (IMAC), where the same type of binding is employed. Typically, in IMAC the optimal ligand density depends on the protein being used [2]. Here, we examine a bovine serum albumin (BSA) that has a low density of naturally exposed histidines. The importance of histidine interactions with transition-metal ions in biological systems has been known for a long time [3]. An affinity chromatographic method based on this principle, known as immobilized metal affinity chromatography (IMAC), has become the most widely used affinity chromatography technique, and it is especially suitable for the rapid and simple isolation of genetically engineered proteins in research laboratories [4–9].

Our basic idea was to bind the BSA reversibly to the surface of the magnetic nanoparticles. For the magnetic nanoparticles we chose monodispersed maghemite nanoparticles that were stabilized in a dispersion using citric acid. As the anchors for the reversible adsorption of BSA we decided to use Zn (II) rather than, for example, Ni (II) or Cu (II) ions, that otherwise, have higher binding affinities for proteins. This is because the highly redox-active Cu (II) ions frequently promote oxidative radical damage of the protein side chains and cleavage of the protein backbone, while Ni (II) compounds are

* Corresponding author. Tel.: +386 1 476 03 20; fax: +386 1 426 03 00.
E-mail address: miran.gaberscek@ki.si (M. Gaberšček).

1570-0232/$ – see front matter © 2008 Elsevier B.V. All rights reserved.
doi:10.1016/j.jchromb.2008.03.019

established human carcinogens [10] and should be avoided, even in trace amounts.

Here, we show that the attempts to directly decorate maghemite nanoparticles with Zn anchors were unsuccessful. So in order to improve the adsorption of Zn onto the surface, we pre-treated the nanoparticles with a thin layer of silica, which is known to strongly adsorb zinc ions, probably following the mechanism of the triple layer [11]. Finally, to prove the basic concept of the reversibility of the BSA adsorption on Zn anchors, we exposed the particle-bound BSA to different environments (different pH values or different imidazole concentrations) and performed an SDS-PAGE analysis.

2. Experimental

2.1. Synthesis of magnetic nanoparticles

Maghemite nanoparticles were precipitated from an aqueous solution of $FeSO_4$ (0.027 mol/L) and $Fe_2(SO_4)_3$ (0.0115 mol/L) with a concentrated ammonia solution (25%) in a two-step process. In the first step, the pH value of the solution was increased to pH 3 and maintained at a constant value for 30 min to precipitate the iron hydroxide. In the second step, the pH value was further increased to pH 11.6. In this step we expected that the iron (II) hydroxide would be oxidized by the oxygen from the air, forming a spinel product. After an aging time of 30 min, the iron oxide particles were magnetically separated and washed several times with a diluted ammonia solution to remove any excess ions. The high pH value of the solution (10.5) provides a very negative surface charge on the nanoparticles, thus preventing their strong agglomeration during the washing.

2.2. Coating the nanoparticles with a thin layer of silica

The surfaces of oxide nanoparticles are chemically relatively inert. Therefore, in order to improve the adsorption of zinc, the nanoparticles were coated with a thin layer of silica by the hydrolysis of tetraethyl orthosilicate (TEOS). In order to homogeneously coat individual nanoparticles and not their agglomerates, the nanoparticles were first dispersed in water using citric acid as a surfactant. Details of the ferrofluid preparation are described elsewhere [12].

In the final stage, the nanoparticles were coated with a thin, homogeneous layer of silica. The pH value of the suspension of particles coated with citric acid was increased to pH 11 using ammonia. Then, 2.5 mL of tetraethylorthosilicate (TEOS) and ethanol (20 wt.%) were introduced into the suspension. After being dissolved in ethanol, the TEOS was introduced into the suspension of magnetic particles, with the mixture being stirred overnight. The hydrolysis and condensation of TEOS – catalyzed by the ammonia present in the ferrofluid – resulted in the nucleation of silica on the surfaces of the nanoparticles. The silica-coated nanoparticles remained in the form of a stable suspension because of the repulsive forces related to the very negative zeta-potential [13].

2.3. Adsorption of Zn on the surfaces of the nanoparticles

For the adsorption of Zn on pure maghemite and silica-coated maghemite nanoparticles, 10 g of a suspension containing 1 wt.% of the nanoparticles was mixed with a given quantity of zinc acetate so that the final concentration in the dispersion was 0.2 mM/L. The final solution had a pH of 8. The mixture was stirred overnight, and then centrifuged for 5 min at 5000 rpm to separate the nanoparticles from the solution. The nanoparticles were then washed with and redispersed in pure water to obtain an approximately 1 wt.% dispersion.

For the adsorption of Zn on pure silica nanoparticles, a 1 wt.% suspension of commercially available silica nanoparticles (Cabosil M5, Riedel de Haen) was first prepared by ultrasonic homogenization for 10 min at room temperature. After that, 0.2 mL of a 5 mmol/L zinc acetate solution was added to the 5 mL of silica suspension. The final mixture was stirred overnight.

2.4. Binding of the BSA on Zn-modified nanoparticles

To bind the bovine serum albumin (BSA) on pure maghemite nanoparticles decorated with zinc, we prepared a 0.5 wt.% solution of BSA at room temperature.

The binding of the BSA on zinc-modified pure silica and on zinc-modified silica-coated maghemite involved mixing 1 mL of a 0.5 wt.% BSA solution with 5 mL of the suspension of the respective nanoparticles. The final mixture, with a pH of 6.5, was stirred overnight.

2.5. Methods for characterizing the materials

The compositions of the nanoparticle suspensions were determined from thermogravimetric measurements. The dried, as-synthesized and the silica-coated nanoparticles were characterized with X-ray powder diffractometry (XRD) (Bruker AXS, D4 ENDEAVOR), and transmission electron microscopy (TEM) (JEOL 2010F) coupled with energy-dispersive X-ray spectroscopy (EDX) (LINK ISIS EDS 300). For the TEM investigations the nanoparticles were deposited on a copper-grid-supported, perforated, transparent carbon foil. The HREM images were taken at the edges of the agglomerated nanoparticles jutting into the hole of the perforated carbon foil. The size of the nanoparticles was estimated from TEM images and using Scherrer's method, based on the broadening of the peaks in the XRD pattern, using Diffrac^{plus} Topas^{TM} software. The specific magnetization of the materials at room temperature was measured using a vibrating-sample magnetometer (LakeShore VSM).

The release of the bound BSA was analysed using sodium dodecyl sulfate polyacrylamide gel electrophoresis (SDS-PAGE). First, 1 ml of solution containing nanoparticles was centrifuged for 10 min at 10,000 rpm. The supernatant was then analysed for unbound BSA. The pelleted nanoparticles were subsequently washed three times with a phosphate buffer (pH 7.2) to wash away all the unbound BSA. After each washing, the nanoparticles were pelleted again by centrifugation at 10,000 rpm for 10 min. The release of the BSA was experimentally confirmed after 30 min of moderate shaking at room temperature after the addition of 0.5 ml of a phosphate buffer (pH 4.5), or a phosphate buffer (pH 7.2) with a 100-mM concentration of EDTA, or a 0.5-M concentration of imidazole, to the pelleted nanoparticles. For the SDS-PAGE analysis, 30 μL of sample was mixed with 10 μL of 4× SDS sample buffer with DTT and denatured for 5 min at 95 °C. The SDS-PAGE was performed according to Laemmli, and the polyacrylamide gels were stained with Coomassie Brilliant Blue.

3. Results and discussion

3.1. Characterization of nanoparticulate inorganic substrates

Three types of nanoparticles were used as the substrates for the protein binding: commercial, pure silica nanoparticles; pure maghemite nanoparticles (stabilized in a dispersion using citric acid); and silica-coated maghemite nanoparticles.

The average size of the commercial, pure amorphous silica nanoparticles, as estimated from TEM images such as that shown in Fig. 1a, was about 20 ± 2 nm.

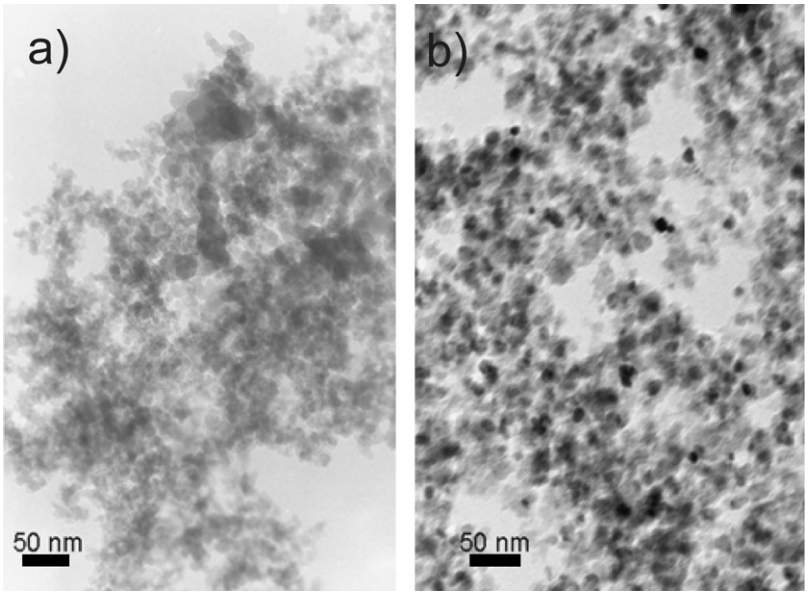

Fig. 1. TEM image of (a) commercial silica nanoparticles and (b) silica-coated maghemite nanoparticles.

The average particle size of the as-synthesized, pure maghemite nanoparticles, estimated from TEM (not shown), was about 15 nm, which was consistent with the value of 13.7 ± 2.9 nm, determined from the broadening of the X-ray diffraction peaks. The X-ray scattering data also revealed a spinel structure which, when combined with a chemical analysis that showed about 3% of iron in oxidation state (II), proves the maghemite nature of these particles.

After coating the maghemite nanoparticles with silica, the average size of the resulting nanocomposites, determined from the TEM, increased to about 18 ± 3 nm. In this present study, the surface distribution of the silica coating was very important, so we performed careful HRTEM studies on these materials. An example is shown in Fig. 2. In this particular case, the silica coating appears to be relatively homogeneous, i.e., it is uniformly spread out over the whole surface of the maghemite. The indicated upper part reveals silica with a thickness of about 1 nm, while the thickness at other parts of the surface could be somewhat less. By performing a similar analysis on many particles, we found that the silica coating was relatively uniform in terms of thickness and that it covered, to a large extent, all the maghemite particles. Based on this analysis, we hypothesized that such silica-coated maghemite nanoparticles should have a similar affinity for zinc adsorption as the pure, commercial silica with a similar particle size.

In the context of possible targeted drug delivery, it was also important to find out to what extent the silica coatings modified the magnetic properties of the maghemite. As can be seen from Fig. 3, neither the magnetization curve recorded before nor that recorded after the coating with silica showed any coercivity, in accordance with the superparamagnetic nature of both materials. The saturation magnetization was found to be 68 emu/g for the as-synthesized nanoparticles and around 37 emu/g for the silica-coated maghemite nanoparticles.

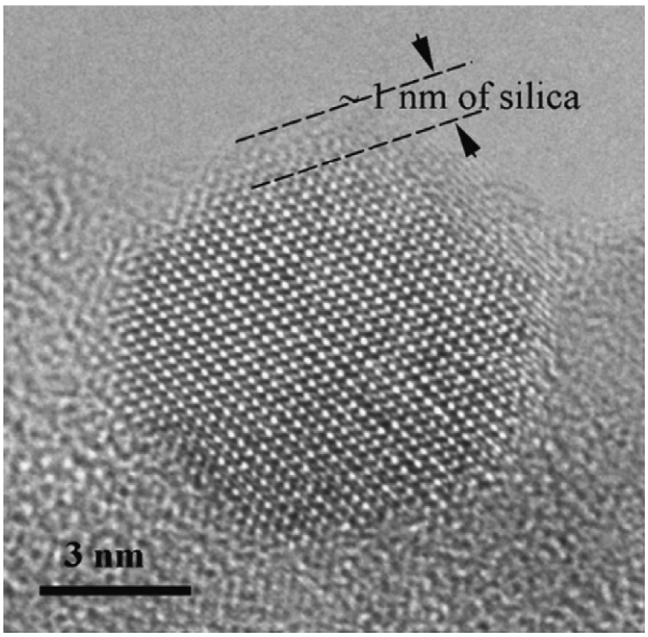

Fig. 2. HREM image of a silica-coated maghemite nanoparticle. The nanoparticle is oriented along the ⟨1 1 0⟩ of its spinel structure. At the surface, an ~1-nm thick amorphous layer of silica is visible.

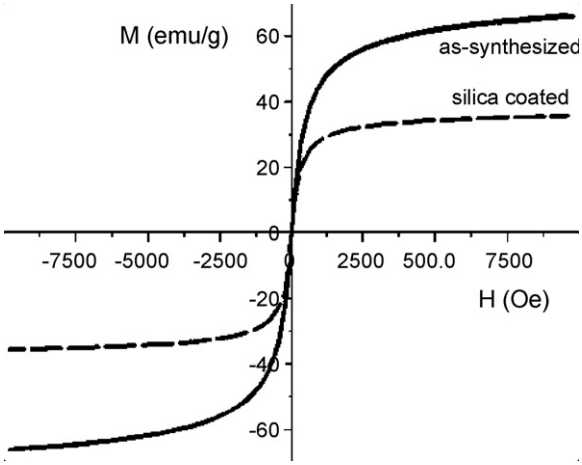

Fig. 3. Room-temperature magnetization hysteresis of as-synthesized nanoparticles and silica-coated nanoparticles.

3.2. Bovine serum albumin binding on various nanoparticulate substrates decorated with zinc

As described in Section 1, the main aim of this present study was to reversibly bind BSA on zinc-decorated maghemite nanoparticles. Here, the zinc species are supposed to serve as the anchor points for the formation of coordinative bonds to the BSA.

In a preliminary experiment, we simply tried to adsorb zinc on the surface of pure maghemite nanoparticles. Remember, however, that in order to keep the maghemite nanoparticles dispersed we had to use an appropriate surfactant, i.e., citric acid. We speculated that the presence of citric acid would negatively affect the zinc adsorption because it is known as a strong complexant for transition elements and, as such, could compete strongly with the maghemite for the zinc. This assumption was indirectly confirmed by performing an SDS-PAGE analysis of the binding of the BSA to the zinc-containing maghemite/citric acid system (Fig. 4). Note that the maghemite nanoparticles were very well dispersed, so it was very difficult to separate them. For example, we had to use ultra-centrifugation at 50,000 rpm for 45 min in order to separate the particles from the unbound BSA. The samples obtained after ultra-centrifugation were then used for the analysis of the binding and the release of the BSA, as described in Section 2 (see also the text of Fig. 5), but the protocol was modified in such a way that all the centrifugation steps were performed with an ultra-centrifuge. As can be deduced from Fig. 4, no BSA was released after the addition of imidazol, which suggests that no BSA was coordinatively bound to this type of particle.

In order to improve the adsorption of zinc, we silica-coated the maghemite nanoparticles. We hoped that the zinc would strongly adsorb on the thin silica layer. Such a zinc-decorated silica-coated nanoparticulate maghemite was then used to study the binding of the BSA using SDS-PAGE analysis (Fig. 5). For an easier interpretation of the results, we also performed the same analysis on zinc-decorated, pure silica of a similar size and size distribution (see Figs. 1–3). Finally, we performed an SDS-PAGE analysis on the two negative (Zn-free) controls: Zn-free silica and Zn-free silica-coated maghemite (Fig. 5).

To exclude unexpected specific effects, we initially checked the release of the BSA with two different methods: by lowering the pH and by the addition of a 0.5-M imidazole. Although the effect was clearly achieved in both cases, we found that the addition of imidazole was more efficient, so this method was used in all the subsequent experiments. After the addition, the imidazole competes with surface-exposed histidine residues on the BSA for binding to the sites containing zinc ions. Due to the high concentration of imidazole, most of the bound BSA was released. As we can see from Fig. 5, the BSA was coordinatively bound to both types of zinc-containing nanoparticles, i.e., to zinc-decorated pure silica and zinc-decorated silica-coated nanoparticles. The intensity of the bands is similar, which indirectly confirms the uniformity of the silica coating around the individual maghemite particles. Most importantly, as we can see from lanes 2 and 7 in Fig. 5, in both cases the BSA was not released after washing with a phosphate buffer of

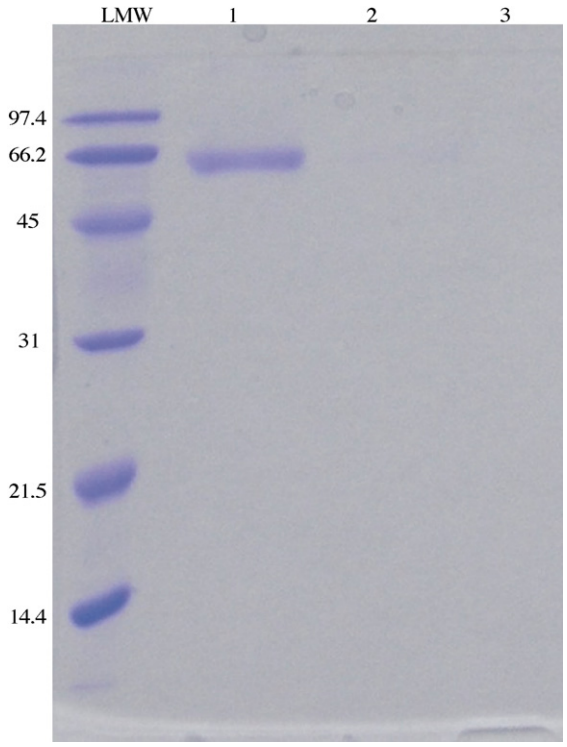

Fig. 4. SDS-PAGE analysis of the binding of the BSA to the zinc-containing maghemite/citric acid nanoparticulate system. LMW (low-molecular weight standards, BioRad), lane 1: unbound BSA, lane 2: washed particles with phosphate buffer of pH 7.2 and lane 3: release of the BSA due to the addition of imidazole.

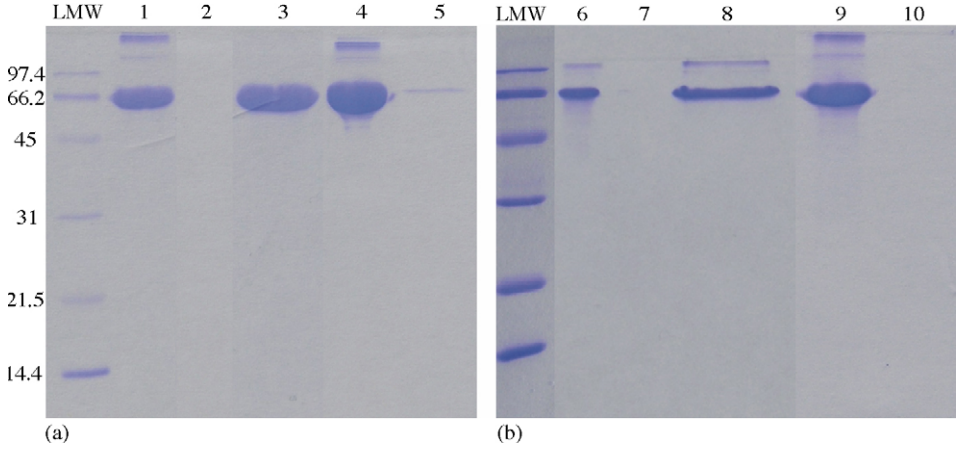

Fig. 5. SDS-PAGE analysis of the binding of the BSA to (a) zinc silica nanoparticles and (b) zinc silica-coated maghemite nanoparticles. Lanes 1–3 represent analyses of the BSA binding to zinc silica nanoparticles and lanes 4 and 5 represent the binding of the BSA to silica nanoparticles without the addition of zinc. Lanes 6–8 show analyses of the BSA binding to zinc silica-coated maghemite nanoparticles and lanes 9 and 10 binding to silica-coated maghemite nanoparticles without the addition of zinc. LMW (low-molecular weight standards, BioRad), lanes 1, 4, 6 and 9 (unbound BSA), lanes 3, 5, 8 and 10 (release of BSA due to addition of imidazole), lanes 2 and 7 (washed particles with phosphate buffer of pH 7.2: no release of BSA).

pH 7.2, but only after the addition of imidazole (lanes 3 and 8), thus proving the reversibility of the binding and the coordinative nature of the bond between the histidine residues in the protein and zinc ions.

That the presence of zinc is essential for any binding of the BSA to the present materials is demonstrated by both the negative controls shown in Fig. 5 (see lanes 4, 5 and 9, 10). In both cases practically no BSA is bound. This proves that no unspecific BSA binding to the present materials occurs if they are not decorated with zinc.

4. Conclusion

A nanometre-thick, uniform, silica coating around magnetic (e.g., maghemite) nanoparticles can serve as an efficient means for the adsorption of transition elements (e.g., zinc) on such modified surfaces. Most importantly, we demonstrated that despite the silica coating, the maghemite nanoparticles preserved their superparamagnetic nature. At pH values between 6.5 and 7.5, the surface density of the adsorbed zinc seems to be high enough to allow for a quantitative and reversible adsorption of model histine-rich proteins such as BSA. By contrast, in the absence of silica, the adsorption of zinc on maghemite was not possible at all.

The nanoparticles investigated in the present work could be interesting for binding and the delivery of therapeutic proteins that are sometimes toxic or cytotoxic in higher doses. With a coordinative type of binding it might be possible to achieve a controlled and/or sustained release of certain protein biopharmaceuticals and maintain a constant and low level of protein in the blood stream or at the specific target site.

Acknowledgements

This work has been financially supported by the Slovenian Research Agency and by the European Commission under the Sixth Framework Programme.

References

[1] A. Frenzel, C. Bergemann, G. Kohl, T. Reinard, J. Chromatogr. B 793 (2003) 325.
[2] J. Liesiene, K. Racaityte, M. Morkeviciene, P. Valancius, V. Bumelis, J Chromatogr. A 764 (1997) 27.
[3] R.J. Everson, H.E. Parker, Bioinorg. Chem. 4 (1974) 15.
[4] J. Porath, J. Carlsson, I. Olsson, G. Belfrage, Nature 258 (1975) 598.
[5] E. Sulkowski, Bioessays 10 (1989) 170.
[6] G.S. Chaga, J. Biochem. Biophys. Methods 49 (2001) 313.
[7] V. Gaberc-Porekar, V. Menart, J. Biochem. Biophys. Methods 49 (2001) 335.
[8] E.K.M. Ueda, P.W. Gout, L. Morganti, J Chromatogr. A 988 (2003) 1.
[9] V. Gaberc-Porekar, V. Menart, Chem. Eng. Technol. 28 (2005) 1233.
[10] W. Bal, H. Kozlowski, K.S. Kasprzak, J. Inorg. Biochem. 79 (2000) 213.
[11] T.N.T. Phan, N. Louvard, S.-A. Bachiri, J. Persello, A. Foissy, Colloid Surf. A 244 (2004) 131.
[12] S. Čampelj, D. Makovec, M. Drofenik, J. Phys.: Condens. Mat., in press.
[13] S. Čampelj, D. Makovec, M. Bele, M. Drofenik, J. Jamnik, MTAEC9 41 (2) (2007) 103.